



Published in final edited form as:

*Biomacromolecules*. 2010 March 8; 11(3): 600–609. doi:10.1021/bm901147k.

## Altering Amine Basicities in Biodegradable Branched Polycationic Polymers for Non-Viral Gene Delivery

Sue Anne Chew<sup>1</sup>, Michael C. Hacker<sup>1,2</sup>, Anita Saraf<sup>1</sup>, Robert M. Raphael<sup>1</sup>, F. Kurtis Kasper<sup>1</sup>, and Antonios G. Mikos<sup>1,\*</sup>

<sup>1</sup>Department of Bioengineering, Rice University, MS-142, P.O. Box 1892, Houston, TX 77251-1892

<sup>2</sup>Department of Pharmaceutical Technology, Institute of Pharmacy, University of Leipzig, Eilenburger Str. 15a, D-04317, Leipzig, Germany

### Abstract

In this work, biodegradable branched polycationic polymers were synthesized by Michael addition polymerization from different amine monomers and the triacrylate monomer trimethylolpropane triacrylate. The polymers varied in the amount of amines that dissociate in different pH ranges, which are considered to be beneficial to different parts of the gene delivery process. P-DED, a polymer synthesized from trimethylolpropane triacrylate and dimethylethylenediamine, had the highest number of protonated amines that are available for pDNA complexation at pH 7.4 of all polymers synthesized. P-DED formed a positive polyplex ( $13.9 \pm 0.5$  mV) at a polymer/plasmid DNA (pDNA) weight ratio of 10:1 in contrast to the other polymers synthesized, which formed positive polyplexes only at higher weight ratios. Polyplexes formed with the synthesized polymers at the highest polymer/pDNA weight ratio tested (300:1) resulted in higher transfection with enhanced green fluorescent protein reporter gene ( $5.3 \pm 1.0\%$  to  $30.6 \pm 6.6\%$ ) compared to naked pDNA ( $0.8 \pm 0.4\%$ ), as quantified by flow cytometry. Polyplexes formed with P-DED (weight ratio of 300:1) also showed higher transfection ( $30.6 \pm 6.6\%$ ) as compared to polyplexes formed with branched polyethylenimine (weight ratio of 2:1,  $25.5 \pm 2.7\%$ ). The results from this study demonstrated that polymers with amines that dissociate above pH 7.4, which are available as positively charged groups for pDNA complexation at pH 7.4, can be synthesized to produce stable polyplexes with increased zeta potential and decreased hydrodynamic size that efficiently transfect cells. This work indicated that polymers containing varying amine functionalities with different buffering capabilities can be synthesized by using different amine monomers and used as effective gene delivery vectors.

### List of Keywords

non-viral gene delivery; biodegradable polymer; ester hydrolysis; amine basicity; molecular weight

### Introduction

Polycationic polymers have been widely investigated as non-viral vectors for gene delivery. In contrast to viral vectors, which are known to be efficient gene carriers, polycationic polymers generally lack drawbacks commonly associated with viral vectors, such as immune response, production complexity and cost<sup>1,2</sup>. Depending on the chemical structure and environment of the amine functionalities in polycationic polymers, these amines dissociate at different pH values resulting in pH dependent charge densities of the polymers. During the various steps

\* Corresponding Author: Antonios G. Mikos, Professor, Department of Bioengineering, Rice University MS-142, P.O. Box 1892, Houston, TX 77251-1892, Tel: (713) 348-5355, Fax: (713) 348-4244, mikos@rice.edu.

involved in the gene delivery process, different buffering profiles are considered to be beneficial. For DNA complexation and polyplex formation, the number of amines dissociating above pH 7.4 is important, as only charged amines are able to electrostatically interact with the negative charges of the phosphate groups along the DNA backbone<sup>3,4</sup>. The process of DNA complexation aids with condensing and protecting plasmid DNA from degradation. An excess of positive charges ultimately results in the formation of positively charged polymer/DNA polyplexes, which can effectively adhere to target cells by interacting with the negatively charged phospholipids and sulfate groups of the proteoglycans on the cells<sup>5,6</sup>. This interaction may also improve the chance for endocytotic internalization of the polymer/DNA polyplexes. Upon internalization, amine functionalities that dissociate in the pH range between 5.0 and 7.4 play an important role, as they buffer the pH in the endosome. A material with buffering capacity in this pH range can assist in the escape of the DNA from the endosome and prevent DNA degradation by nucleases in the lysosome through the proton sponge effect<sup>5</sup>. During the delivery process, an optimal degradation rate of main or side chains is another vital component of the polycationic polymer to ensure the release of the encapsulated pDNA and the excretion of the polymer and its side products<sup>7</sup>. Polymer degradation should not occur too rapidly to avoid premature disassembly of the DNA from the polyplex. On the other hand, the polymer should degrade quickly enough to facilitate DNA disassembly from the polyplex once the polyplex reaches the cytoplasm or nucleus, so that free DNA is available for expression in the nucleus<sup>8</sup>. The degradation of the polymer is also beneficial in lowering the cytotoxicity of the polymer, as the polymer's charge density decreases when the polymer degrades into fragments of low molecular weight, which interact less with cell compartments<sup>9,10</sup>. It has been shown for poly(ester amine)s that unprotonated amines have the capability to autocatalyze degradation<sup>11</sup>. Thus, for poly(ester amine)s, amine groups that are in an unprotonated state at pH 5.0 (lysosomal pH) and 7.4 (cytoplasmal pH) play important roles during the delivery process.

Biodegradable polycationic polymers can be synthesized by different polymerization methods, such as Michael addition<sup>12-19</sup> and reversible addition-fragmentation chain transfer (RAFT)<sup>20,21</sup> polymerization. Biodegradable polymers synthesized from acrylate and amine monomers by Michael addition polymerization as non-viral gene delivery vectors have been previously investigated by many groups, including ours. The acrylate monomers can be either bifunctional<sup>12-15</sup> or trifunctional<sup>16-19</sup> yielding linear or branched poly(ester amine)s, depending on the type of amine monomer used during the addition reaction. The ester groups in the acrylate monomers allow for hydrolytic biodegradation of the polymers. In our previous work, we synthesized a series of polymers with different types of triacrylate monomers and with a single amine monomer, 1-(2-aminoethyl)piperazine (AEPZ), to investigate the effects of hydrophilic spacer lengths on polymer properties relevant for the gene delivery process<sup>19</sup>. It was found that the incorporation of hydrophilic spacers into the polymers decreased polymer cytotoxicity and accelerated hydrolytic degradation. These alterations of the triacrylate monomer chemistry, however, resulted in a decrease of amine group density and affected the contribution of the amines to key steps of the gene delivery process, namely DNA complexation, endosomal escape and polymer degradation. In addition, variations of the hydrophilicity of the triacrylate monomers did not significantly affect the dissociation properties of the polymers. Consequently, this study focuses on altering the amine monomers used during polymer synthesis with the objective to yield polymers with buffering profiles and pKa values different from those investigated in our previous work<sup>19</sup>. It is hypothesized that by changing the density, degree of substitution and chemical environment of the polymeric amine groups through altering the amine monomers used for polymer synthesis, polymer characteristics relevant for gene delivery can be altered and controlled.

In this study, a series of polymers was synthesized by chemically conjugating different amine monomers with a single triacrylate monomer, trimethylolpropane triacrylate (TMPTA), to

evaluate the effects of altering amine basicities on parameters important for gene delivery. The specific objectives of this work were to investigate the effects of chemically different amine groups on characteristics of the polymer synthesized (molecular weight, basicity determined as amine equivalents dissociating within different pH ranges, degradability and cytotoxicity) and of polyplexes with plasmid DNA (pDNA) (polyplex hydrodynamic diameter, zeta potential and transfection efficiency) to determine design parameters for effective non-viral gene delivery vectors.

## Materials and Methods

### Materials

TMPTA, AEPZ, 1-(3-aminopropyl) imidazole (API), N,N-dimethylethylenediamine (DED), Hydrazine (Hyd), branched polyethylenimine (PEI) (typical weight average molecular weight,  $M_w \sim 25$  kDa, polydispersity index (PDI) of 2.5), chloroform (ACS grade), sterile-filtered dimethyl sulfoxide (DMSO), methyl tetrazolium (MTT) powder, phenol red free Dulbecco's modified Eagle medium (DMEM), ethidium bromide and Tris-Acetate-EDTA (TAE) were purchased from Sigma-Aldrich (St. Louis, MO). Deuterium oxide ( $D_2O$ ) was obtained from Cambridge Isotope Laboratories, Inc. (Andover, MA). Acetone (ACS grade), isopropanol (ACS grade) and Fisher Certified Buffer pH 5.0 and 7.4 were purchased from Fisher Scientific (Pittsburgh, PA). Fischer rat fibroblast 3T3-like cell line (CRL 1764) was obtained from American Type Culture Collection (Manassas, VA). DMEM and phosphate-buffered saline (PBS) were purchased from Gibco Life (Grand Island, NY). Fetal bovine serum (FBS) was obtained from Gemini Bio-Products (Calabasas, CA). Trypsin-ethylenediaminetetraacetic acid (EDTA) (0.25% trypsin/0.02% EDTA) was obtained from Invitrogen (Carlsbad, CA). Poly (ethylene glycol) (PEG) standards with  $M_n$  ranging from 102 to 82,500 Da used for SEC were obtained from Waters (Milford, PA). Plasmid DNA (pDNA) with a cytomegalovirus (CMV) promoter and enhanced green fluorescent protein (eGFP) reporter gene (pCMV-eGFP, 4.7 kb, cat no. 6085-1) was obtained from Clontech (Palo Alto, CA). Qiagen Endofree Plasmid Giga Kit was purchased from Qiagen (Valencia, CA).

### Synthesis

**Synthesis at Room Temperature (P-AEPZ)**—P-AEPZ (Table 1) was synthesized by reacting AEPZ with TMPTA as previously described<sup>18,19</sup>. Briefly, the polymer was synthesized at a 2:1 mole ratio<sup>16-18</sup> of amine to triacrylate monomer in chloroform. The mixture was allowed to react for 8 days under ambient temperature and then purified by precipitation in a solution of 400 mL of acetone and 5 mL of hydrochloric acid (HCl) (12 M). The product was washed with excess acetone and finally vacuum dried to remove any remaining solvent. The <sup>1</sup>H-NMR spectra revealed the following characteristic signals: **P-AEPZ**:  $\delta$  0.9 (t, C-CH<sub>2</sub>-CH<sub>3</sub>), 1.4 (m, C-CH<sub>2</sub>-CH<sub>3</sub>), 2.5–3.5 (t, -CH<sub>2</sub>-CH<sub>2</sub>-NR<sub>2</sub>- and t, -CH<sub>2</sub>-CH<sub>2</sub>-COO-CH<sub>2</sub>-), 4.0–4.1 (s, C-CH<sub>2</sub>-OOC-CH<sub>2</sub>-).

**Synthesis at 50°C (P-API, P-DED, P-Hyd, P-AEPZ/Hyd and P-API/Hyd)**—All other polymers (Table 1) were synthesized by reacting TMPTA with API (P-API), DED (P-DED), Hyd (P-Hyd), AEPZ and Hyd (1:1 mole ratio) (P-AEPZ/Hyd) and API and Hyd (1:1 mole ratio) (P-API/Hyd) on the basis of previous methods<sup>16,17</sup>. The polymers were synthesized at a 2:1 mole ratio of amine to triacrylate monomer. Typically, 10.8 mmole of the amine monomer and 5.4 mmole of the triacrylate monomer were mixed in 20 mL of chloroform in a round bottom flask. For P-AEPZ/Hyd and P-API/Hyd, 5.4 mmole of each type of amine monomer was used, which resulted in a total of 10.8 mmole of amine monomer. The mixture was allowed to react for 3 days at 50°C. The polymer was then purified by precipitation in a solution of 400 mL of acetone and 5 mL of concentrated hydrochloric acid (12 M). The product was washed with excess acetone and finally vacuum dried to remove any remaining solvent. The <sup>1</sup>H-NMR

spectra revealed the following characteristic signals: **P-DED**:  $\delta$  0.9 (t, C-CH<sub>2</sub>-CH<sub>3</sub>), 1.4 (m, C-CH<sub>2</sub>-CH<sub>3</sub>), 2.5–3.7 (t, -CH<sub>2</sub>-CH<sub>2</sub>-NR<sub>2</sub>-, s, -CH<sub>3</sub>-N- and t, -CH<sub>2</sub>-CH<sub>2</sub>-COO-CH<sub>2</sub>-), 4.0–4.1 (s, C-CH<sub>2</sub>-OOC-CH<sub>2</sub>-). **P-Hyd**:  $\delta$  0.9 (t, C-CH<sub>2</sub>-CH<sub>3</sub>-), 1.4 (m, -CH<sub>2</sub>-CH<sub>3</sub>-), 2.3–3.6 (t, -CH<sub>2</sub>-CH<sub>2</sub>-NH-NH- and t, -CH<sub>2</sub>-CH<sub>2</sub>-COO-CH<sub>2</sub>-), 4.0–4.1 (s, C-CH<sub>2</sub>-OOC-CH<sub>2</sub>-). **P-AEPZ/Hyd**:  $\delta$  0.9 (t, C-CH<sub>2</sub>-CH<sub>3</sub>), 1.4 (m, C-CH<sub>2</sub>-CH<sub>3</sub>), 2.5–3.6 (m, -CH<sub>2</sub>-CH<sub>2</sub>-NR<sub>2</sub>, t, -CH<sub>2</sub>-CH<sub>2</sub>-NH-NH- and t, -CH<sub>2</sub>-CH<sub>2</sub>-COO-CH<sub>2</sub>-), 4.0–4.1 (s, C-CH<sub>2</sub>-OOC-CH<sub>2</sub>-). **P-API/Hyd**:  $\delta$  0.9 (t, C-CH<sub>2</sub>-CH<sub>3</sub>), 1.4 (m, C-CH<sub>2</sub>-CH<sub>3</sub>-), 2.1 (m, -NR<sub>2</sub>-CH<sub>2</sub>-CH<sub>2</sub>-CH<sub>2</sub>-NR<sub>2</sub>-), 2.1–3.5 (t, -CH<sub>2</sub>-CH<sub>2</sub>-NR<sub>2</sub>-, t, -CH<sub>2</sub>-CH<sub>2</sub>-NH-NH- and t, -CH<sub>2</sub>-CH<sub>2</sub>-COO-CH<sub>2</sub>-), 4.0–4.1 (s, C-CH<sub>2</sub>-OOC-CH<sub>2</sub>-). 4.3 (t, -CH<sub>2</sub>-CH<sub>2</sub>-imidazole-), 7.2–7.4 (d, -N-CH=CH-N-), 8.3 (s, -N=CH-N-).

## Polymer Characterization

The results reported for P-AEPZ in this study (i.e., polymer molecular weight, hydrogen ion titration and ester degradability and polymer/pDNA polyplex zeta potential, band retardation and hydrodynamic diameter) are adopted from a previous study (represented as P-OE/M)<sup>19</sup>. Experiments that involve cells (i.e., cytotoxicity and transfection efficiency studies) were repeated to avoid variations between different cell pools.

**Proton Nuclear Magnetic Resonance (<sup>1</sup>H-NMR)**—<sup>1</sup>H-NMR spectra of the polymers were obtained using a 400 MHz Bruker spectrometer (Bruker Avance 400, Zurich, Switzerland). The samples were dissolved in deuterium oxide (D<sub>2</sub>O) and the resulting spectra were analyzed using MestRe-C, a NMR processing software package (Mestrelab Research S. L., Spain). The proton peak of deuterium protium oxide (HDO) was used as the internal shift reference and therefore set to  $\delta$  = 4.8 ppm.

**Molecular Weight Determination by Size Exclusion Chromatography (SEC)**—The weight average molecular weight (M<sub>w</sub>), number average molecular weight (M<sub>n</sub>) and polydispersity index (PDI) (M<sub>w</sub>/M<sub>n</sub>) of the polymers were determined by SEC using a Waters Alliance<sup>®</sup> HPLC system (Waters, Milford, PA) equipped with a differential refractometer as previously described<sup>19</sup>. Briefly, the samples were run through a Shodex OHpak SB-G (6.0 × 50 mm) guard column, a Shodex OHpak SB803 HQ (8.0 × 300 mm) and a Shodex OHpak SB802.5 HQ (8.0 × 300 mm) analytical column placed in series using PEG standards with M<sub>n</sub> ranging from 102 to 82,500 Da to obtain a calibration curve (as previously done by Wu et al.<sup>18</sup> and our group<sup>19</sup> for polymers with similar architecture to those synthesized in this study). A 0.5 M sodium acetate buffer containing 0.1 M sodium nitrate was used as the mobile phase (pH 4.5) with a flow rate of 0.5 mL/min. The theoretical average compositions of the polymers were calculated as previously described<sup>19</sup>.

**Hydrogen Ion Titration**—The number of amine equivalents in a given mass of polymer was evaluated by hydrogen ion titration as done previously<sup>19</sup>. Briefly, 50 mg of polymer were dissolved in 10 mL of 150 mM sodium chloride (NaCl) solution. The polymer solution was adjusted to a pH of 2.0 and then titrated by stepwise addition of 0.1 N NaOH while measuring the pH of the solution using an accumet<sup>®</sup> AP63 Portable pH meter (Fisher Scientific, Pittsburgh, PA). Each titration was done in triplicate, and average pH values were calculated and reported. The amine equivalents that dissociated in different pH ranges were determined as previously described<sup>19,22</sup>. The pK<sub>a</sub> values were obtained from the titration curves as the pH values at 50% ionization or half way to the equivalent point (midpoint of the plateau areas on the curves).

**Polymer Degradation by <sup>1</sup>H-NMR Analysis**—The rate of hydrolytic ester degradation of the different polymers was determined at pH 5.0 and 7.4 by <sup>1</sup>H-NMR analysis as described previously<sup>18,19,23,24</sup>. Briefly, a polymer sample (7.5 mg) was dissolved in 750  $\mu$ L of Fisher Certified Buffer pH 5.0 or pH 7.4<sup>25</sup> and incubated at 37°C with constant agitation (75 rpm).

At predefined time points (0 h, 6 h, 12 h, 1 d, 3 d, 7 d and 14 d), the samples were analyzed by  $^1\text{H-NMR}$ . This study was done in triplicate ( $n=3$ ). At each time point, percent ester degradation was calculated as previously described<sup>19</sup>.

**Cytotoxicity Analysis by MTT Assay**—The cytotoxicity of the polymers was evaluated using an MTT viability assay as described previously<sup>19,26</sup>. Briefly, CRL 1764 rat fibroblasts were plated on 96-well plates with a density of 8000 cells/well. Polymer solutions with a pH of 7.4 and an osmolarity of 280–320 mosm/kg were prepared in DMEM at six different polymer concentrations (10, 50, 100, 250, 500 and 1000  $\mu\text{g/mL}$ ). Branched PEI ( $M_w \sim 25$  kDa) solutions at the same concentrations were used as negative controls. Branched PEI 25 kDa has been widely evaluated and is often used as a control for cytotoxicity studies by other groups in the literature<sup>18,27</sup>. After 24 h of cell attachment, the cells were incubated for 2 and 24 h at 37°C in the presence of 100  $\mu\text{L}$  of the polymer solution. MTT assay was performed immediately after the two time points and the absorbance was measured at 570 nm using an absorbance microplate reader (Powerwave X340, BIO-TEK Instruments, Winooski, VT). The average number of live cells was calculated from 5 different samples as previously described<sup>19</sup>.

### Polymer/pDNA Polyplex Characterization

**Amplification and Purification of Plasmid DNA**—pCMV-eGFP was amplified in *Escherichia coli* (*E. coli*) bacterial cultures and purified using a Qiagen Endofree Plasmid Giga Kit according to the protocols provided by the manufacturer. The yield of pDNA was determined from the UV absorbance at a wavelength of 260 nm ( $A_{260}$ ) (NanoDrop™ 1000 Spectrophotometer, Thermo Scientific, Wilmington, DE). To evaluate plasmid purity, the ratio of the UV absorbance at wavelengths of 260 nm and 280 nm ( $A_{260}/A_{280}$ ) was determined and found to range between 1.8 and 2.0. The pCMV-eGFP plasmid was used in all of the polymer/pDNA polyplex characterization experiments.

**Zeta Potential**—The zeta potential of polymer/pDNA polyplexes at different polymer to pDNA weight ratios (5:1, 10:1, 50:1, 100:1, 200:1 and 300:1) was obtained as previously described<sup>19</sup>. Briefly, the polyplexes were prepared with 10  $\mu\text{g}$  of pDNA in 600  $\mu\text{L}$  PBS. The zeta potential of the resulting particles or larger aggregates was obtained using a Zen 3600 Zetasizer (Malvern Instruments, Worcestershire, UK) at 25°C. The zeta potential was calculated using the Smoluchowski equation based on the electrophoretic mobility<sup>28</sup>. This study was done in triplicate.

**Band Retardation with Gel Electrophoresis**—Band retardation of the polyplexes at different weight ratios (10:1, 20:1, 30:1, 40:1, 60:1, 80:1 and 100:1) of polycationic polymer to pDNA solutions was performed as previously described<sup>19</sup>. Briefly, the polyplexes were prepared from 1  $\mu\text{g}$  pDNA in 20  $\mu\text{L}$  PBS and loaded into the wells of a 0.5% (w/w) agarose gel with bromophenol blue loading solution. The gel was run for 1 h at 80 mV in TAE buffer (1 $\times$ ) and an image of the gel was captured in a UV transillumination box.

**Hydrodynamic Polyplex Sizes by Dynamic Light Scattering (DLS)**—The hydrodynamic diameter of the polycationic polymer/pDNA polyplexes was evaluated at different polymer to pDNA weight ratios (10:1, 50:1, 100:1, 200:1, 300:1 and 500:1) using a 90PLUS Particle Size Analyzer (Brookhaven Instruments Corporation, Holtsville, NY)<sup>19</sup>. In brief, the polyplexes were prepared with 10  $\mu\text{g}$  pDNA in 600  $\mu\text{L}$  of PBS and analyzed in the instrument. The diameter of the polyplexes or aggregates thereof was obtained using Laplace inverse program Non-Negative Least-Squares (NNLS)<sup>27</sup>. This study was done in triplicate.

**eGFP Transfection of Rat Fibroblasts**—The transfection of CRL 1764 rat fibroblasts was performed as previously described<sup>19</sup>. Rat fibroblasts were plated in 6-well plates at a

seeding density of 250,000 cells/well. After 24 h of cell attachment, the cells were incubated in the presence of 100  $\mu\text{L}$  of polyplex solution containing 5  $\mu\text{g}$  of pDNA complexed at different polymer/pDNA weight ratios (10:1, 50:1, 100:1, and 300:1) and 400  $\mu\text{L}$  of DMEM (FBS free). PEI/pDNA at a weight ratio of 2:1, naked pDNA and FBS-free media without pDNA served as controls. After 24 h, the cells were supplemented with 2 mL of DMEM/FBS (10% (v/v)) which resulted in a solution containing 8% instead of 10% (v/v) of FBS. The slightly lower concentration of FBS was not expected to significantly affect the metabolism of the cells. After 48 h, the cells were then trypsinized and fixed with chilled formaldehyde solution (1%). Samples were then analyzed using a flow cytometer (Becton Dickinson FACS Scan, BD Biosciences, San Jose, CA). This study was conducted with  $n=6$ . Fluorescence images of selected samples were taken with a confocal microscope (Zeiss LSM 510, Carl Zeiss Jena, Germany) to confirm transfection and expression of the green fluorescent protein (GFP). The cells were imaged with a 20 $\times$  objective after excitation by an argon laser. We ensured that the highest weight ratios tested in the transfection study had a lower mass of polymer per unit area of culture well (150  $\mu\text{g}/\text{cm}^2$ , weight ratio of 300:1) compared to that tested in the cytotoxicity experiment. In the cytotoxicity experiment, cells exposed to the highest mass of polymer per unit area of culture well tested, 300  $\mu\text{g}/\text{cm}^2$  (polymer concentration of 1000  $\mu\text{g}/\text{mL}$ ), were still viable.

### Statistical Methods

The results were presented as means  $\pm$  standard deviation. Multiple-factor analysis of variance (ANOVA) was used to identify if there were any significant differences among groups ( $p < 0.05$ ). Tukey's Honestly Significantly Different (HSD) test was then conducted to identify the specific groups that differed statistically significantly.

## Results and Discussion

### Synthesis

A series of polymers were synthesized and precipitated in acetone/HCl. The sticky precipitates were solid, rubbery or a viscous liquid. In their protonated form, the polymers were insoluble in organic solvents, thus all characterizations were done in aqueous media. An exemplary structure of the synthesized branched polymers is shown in Figure 1 with DED as the amine monomer.

Different synthesis methods (room temperature/non-heated or heated) had to be applied to yield the different polymers. P-AEPZ was obtained at ambient temperature. If polymerized at 50 $^\circ\text{C}$ , the reaction solution of P-AEPZ formed a cross-linked gel. All other polymers were synthesized at an elevated temperature (50 $^\circ\text{C}$ ) because reactions at room temperature were incomplete, as indicated by the presence of olefinic proton signals (5.8-6.6 ppm) in the  $^1\text{H}$ -NMR spectra of the final products. The synthesis of P-API was incomplete even when the synthesis was performed at temperatures above 50 $^\circ\text{C}$  or at increased reaction time and amine monomer concentration. Any unreacted acrylate groups in P-API could possibly contribute to polymer toxicity<sup>29</sup>, thus P-API was excluded from further characterizations. The synthesis of P-Hyd was complete with regard to acrylate group conversion (no olefinic proton peaks present), however, the polymeric product only dissolved in acidic solutions. Thus, P-Hyd was only characterized by hydrogen ion titration. The yields of the polymerization were between 80-90%.

The obtained  $^1\text{H}$ -NMR data were also used to verify that the polymer building blocks, amine and triacrylate monomer, reacted at the intended molar ratio of 2:1, which represents the monomer ratio at initiation. The integral of the signals between 2.5–3.5 ppm (derived from  $-\text{CH}_2-\text{CH}_2-\text{NR}_2-$  (of the amine monomers AEPZ, API, DED),  $\text{H}_3\text{C}-\text{NR}_2-$  (of DED),  $-\text{CH}_2-$

$\text{CH}_2\text{-NR}_2\text{-}$  formed through the reaction, and  $\text{-CH}_2\text{-COO-CH}_2\text{-}$  from the triacrylate monomer) was compared to the integral of the proton signal at 0.9 ppm (derived from three methyl protons in the triacrylate monomer). The calculations yielded molar ratios for P-AEPZ, P-DED, P-AEPZ/Hyd and P-API/Hyd of 1.8, 2.3, 2.5, and 1.7, respectively.

## Polymer Characterization

**Molecular Weight with Size Exclusion Chromatography**—The  $M_n$ ,  $M_w$  and PDI of the polymers as obtained by SEC as well as the theoretical average composition of the polymers calculated based on the experimental  $M_n$  and  $M_w$  values are shown in Table 2. P-AEPZ, which on average consists of 4 triacrylate and 8 amine monomers, had a higher molecular weight ( $M_n$  of 2700 Da) compared to the other polymers which on average consisted of only 2 triacrylate and 4 amine monomers ( $M_n < 1000$  Da). Only P-AEPZ was synthesized at room temperature, while all other polymers were synthesized at 50°C, which may have contributed to the observed differences in molecular weight and monomer composition. Another possible explanation for the different degrees of polymerization may be the different reactivity of the amine monomers used<sup>13</sup>. Low molecular weights were obtained for the synthesized polymers. The molecular weights of the polymers were obtained with SEC using linear PEG standards to generate the calibration curve. The calibration with a linear polymer may not account for the effect of branching that may be present in the polymers; thus an underestimation of the molecular weights may have occurred. The molecular weight<sup>30</sup> and degree of branching<sup>31</sup> of polymers are factors that can highly affect the parameters of non-viral gene delivery polymers which in turn can affect their transfection efficiencies.

**Determination of Buffering Profiles and Polymer pKa Values by Hydrogen Ion Titration**—Hydrogen ion titration of the polymers was started at pH 2 with sodium hydroxide until a pH of 12 was reached, in order to avoid degradation of the polymers at basic pH. The obtained titration curves are shown in Figure 2. Table 2 summarizes the pKa values that were determined for the synthesized polymers. The building block AEPZ has a primary, secondary and tertiary amine and a specified pKa value of 9.30. API has a primary amine with a pKa of 9.81 and a basic imidazole amine with a pKa of 6.28. Imidazole polymers have been shown to exhibit buffering capacity in the endosomal/lysosomal pH range and are often incorporated into polymers as endosomal escape moieties<sup>4,32,33</sup>. The ethylenediamine group in DED, used previously by Kim et al.<sup>16,17</sup>, is a diacid molecule and forms a 5-membered ring with a gauche-anti conformational transition upon protonation<sup>34</sup>, which results in pKa values of 9.74 and 6.36. Xiong et al. have synthesized a polymer containing hydrazide moieties, which are characterized by a low pKa of around 5.00 and therefore remain predominantly uncharged at physiological pH<sup>35</sup>. Xiong et al. found that polymeric hydrazide moieties do not participate in the proton sponge effect due to the low pKa<sup>35</sup>. These functionalities, however, may be beneficial for poly(ester amine) degradation. Amines with low pKa values, which remain unprotonated at pH 5.0 or 7.4, can autocatalyze the degradation of esters at that pH<sup>11</sup>. In this work, we found that the pKa value of hydrazine decreased from 7.97 (monomer) to 4.24 upon conversion into a higher order amine during polymerization (P-Hyd).

In general, the pKa values of the amines (Table 2) changed upon conversion in the Michael addition reaction as a result of the increase in alkyl substitution during the reaction. Sterically hindered accessibility also contributes to the observed changes in the pKa values of the amines. The molecular weight and degree of branching of the polymers could also affect the dissociation of the amines. As seen in Table 1, the polymers that were synthesized cover a wide range of pKa values as intended by the choice of the different amine monomers. P-AEPZ had a single pKa of 7.85. Through the addition of amines from amine monomers DED, Hyd and API, polymers were produced that contained amine groups with pKa values above and below 7. The incorporation of the amine monomer DED resulted in a polymer (P-DED) with two pKa values,

9.56 for the primary amine of the monomer, which could have become secondary or tertiary upon polymerization, and 5.56 for the tertiary amine that dissociates through the gauche-anti conformational transition. The incorporation of the amine monomer API in P-API/Hyd resulted in a pKa of 8.96 for the primary amine of the monomer, which could have become secondary or tertiary upon polymerization, and an additional, low pKa value of 6.32 for the imidazole amine. The amine monomer Hyd which was incorporated into P-Hyd, P-AEPZ/Hyd and P-API/Hyd, resulted in an additional low pKa value of 4.24, 6.34 and 4.14, respectively. By incorporating two different amine monomers in the polymer, such as in P-AEPZ/Hyd and P-API/Hyd, the resulting polymers displayed multiple pKa values covering a wide pH range.

The titration curves for the four different polymers were all different in shape (Fig. 2), which demonstrates that the type of amine monomer had a significant effect on the buffering capacity and profile of the polymers. In contrast, polymers made from the same type of amine monomer (AEPZ), were very similar in shape<sup>19</sup>.

The amine equivalents dissociating in four different pH ranges were evaluated for a given mass of polymer (typically: 50 mg) as done in previous work<sup>19</sup> (Fig. 3). The amine equivalents that dissociate between pH 2.5 - 5.0 and pH 2.5 - 7.4 were evaluated in order to compare the availability of unprotonated amines, which may catalyze the degradation at pH 5.0 and 7.4, respectively<sup>11</sup>. The amine equivalents that dissociate at pH 5.0 - 7.4 were obtained to evaluate the buffering capacity of the polymers at the endosomal/lysosomal pH range, which determines the polymer's ability to aid in pDNA escape from the endosome prior to lysosomal degradation by nucleases<sup>6</sup>. The amine equivalents dissociating between pH 7.4 - 11.0 are charged at physiological pH and considered to aid in polymer/pDNA polyplex formation at pH 7.4.

For a given mass of polymer (50 mg), P-AEPZ had the highest buffering capacity in the range relevant to assist in endosomal escape (pH 5.0-7.4) as compared to the other polymers (Fig. 3). Compared to P-AEPZ, the other polymers (P-DED, P-AEPZ/Hyd and P-API/Hyd) had significantly more amines dissociating in the pH range of 2.5 to 5.0. Such amine groups can help catalyze polymer degradation at pH 5.0. P-AEPZ and P-API/Hyd had the highest amount of amines that may assist with the catalysis of hydrolytic degradation at pH 7.4 compared to the other polymers. Compared to all other polymers, P-DED had a significantly higher number of amines dissociating between pH 7.4 and 11 - dissociation above pH 7.4 is important for polyplex assembly at this pH. The high pKa values of P-DED and P-AEPZ/Hyd were similar (9.56 and 9.61, respectively), however, the buffering profiles of the polymers at pH 7.4 (cytoplasmal pH) are significantly different. This demonstrates that it is not only important to compare the pKa values of the polymers, but also the buffering profiles and amount of amine equivalents at the different pH ranges. The data in Figure 3 also illustrates that the different polymers synthesized from various amine monomers, which resulted in different molecular weights and molar contents of amine groups, significantly varied in the amine equivalents dissociating in the four investigated pH ranges. When the triacrylate monomer chemistry was varied, as done in our previous work, the amount of amine equivalents dissociating in the four investigated pH ranges decreased as the hydrophilic spacer length increased and did not vary significantly between the different pH ranges<sup>19</sup>.

**Polymer Degradation with <sup>1</sup>H-NMR Analysis**—The degradation profiles of the different polymers at pH 5.0 and 7.4 are shown in Figure 4A and 4B, respectively. Figure 4C compares the polymers at two different time points (3 and 14 days). Even though P-DED, P-AEPZ/Hyd and P-API/Hyd had more unprotonated amines at pH 5.0 (Fig. 3), their rates of degradation at day 3 were still significantly lower than those observed for P-AEPZ at pH 5.0 (Fig. 4C). P-DED, P-AEPZ/Hyd and P-API/Hyd may have formed polymers with structures in which the polymer chains are not as flexible, thus, the unprotonated amines in the polymers are less likely to interact with the ester groups and catalyze the degradation of the polymers. Furthermore, P-



AEPZ may have formed a polymer with more accessible ester groups. P-DED, P-AEPZ/Hyd and P-API/Hyd may have more hidden ester groups, which can result in the reduction in the rate of hydrolysis<sup>36</sup>. The results from this study suggest that although a polymer has a higher amount of amines that may autocatalyze degradation, other factors, such as accessibility of the ester groups and flexibility of the polymer chains to allow for the interaction of the unprotonated amines and ester groups, may also affect hydrolysis and result in a lower degradation rate. Further studies that investigate the polymer architecture and topology will give a better understanding regarding the differences in degradation rates seen in this study. P-AEPZ/Hyd achieved around the same amount of degradation as P-AEPZ by day 14 (~45% and 90% at pH 5.0 and 7.4, respectively). ~80% of the esters in P-AEPZ degraded after 3 days and ~80% of the esters in P-DED degraded after 14 days at pH 7.4. These two polymers will be good candidates for evaluating pDNA release kinetics from polycationic polymers with a high (P-AEPZ) and low (P-DED) degradation rate. A higher rate of degradation was seen for all the polymers at pH 7.4 (cytoplasmal pH) than at pH 5.0 (lysosomal pH). This resulted from the higher number of unprotonated amine groups that are present at the higher pH to catalyze hydrolysis of the ester groups, which is consistent with previous work on poly(ester amine)<sup>11,19,37</sup>.

**Cytotoxicity Analysis**—Cells remained viable after incubation with the synthesized polymer solutions for 2 and 24 h at all tested concentrations. More than 85% of the cells exposed to the different synthesized polymers were viable at all concentrations (Fig. 5). In contrast, PEI caused significant cell death after 2 h with less than 12% cell viability at a concentration of 250  $\mu\text{g}/\text{mL}$  and higher and after 24 h with less than 6% cell viability at a concentration of 10  $\mu\text{g}/\text{mL}$  and higher. PEI (25 kDa) has a molecular weight which is 9 times higher than that of P-AEPZ and around 30 times higher than that of all other polymers. Furthermore, PEI has a charge density which is approximately 2 times higher compared to the polymers synthesized in this study. The high toxicity of PEI may have resulted from these two parameters<sup>32,38</sup>. The improved cytocompatibility of the developed polycationic polymers will allow for the use of these polymers at high concentrations and high N:P ratios. Especially P-DED, which contains a considerable amount of amines that dissociate at and above pH 7.4 and is therefore strongly charged at this pH, and showed good cytocompatibility even when exposed to cells at concentrations as high as 1000  $\mu\text{g}/\text{mL}$ .

### Polymer/pDNA Polyplex Characterization

**Zeta Potential**—The optimal polymer to pDNA ratios are those which result in a polyplex with a positive surface charge that allows the polyplex to interact with the negative charges on the cell membrane<sup>5,39</sup>. The pCMV-eGFP plasmid, which was used in this study, has a zeta potential of  $-33.1 \pm 0.5$  mV. All the polyplexes formed at a polymer/pDNA weight ratio of 5:1 had a negative zeta potential ranging between  $-8.5$  and  $-30.0$  mV (Fig. 6). At a weight ratio of 10:1, P-AEPZ and P-DED formed polyplexes characterized by a zeta potential of  $0.0 \pm 0.0$  mV and  $13.9 \pm 0.5$  mV, respectively. P-AEPZ/Hyd and P-API/Hyd, which contain a lower number of amines per weight of polymer that are protonated at pH 7.4 and that can participate in pDNA complexation as compared to P-AEPZ and P-DED (Fig. 3), formed negative polyplexes at a weight ratio of 10:1 and positive polyplexes at a weight ratio of 50:1. Half of the amine monomers in P-AEPZ/Hyd (synthesized from a 1:1:1 mole ratio of TMPTA:AEPZ:Hyd) and P-API/Hyd (synthesized from a 1:1:1 mole ratio of TMPTA:API:Hyd) are derived from hydrazine, which is characterized by a low pKa once incorporated into the polymers. Thus, the amines will not be protonated at physiological pH (7.4) and therefore cannot contribute to the complexation of pDNA. As a result, a higher polymer to pDNA ratio is needed for P-AEPZ/Hyd and P-API/Hyd to neutralize the charges of the pDNA as compared to P-AEPZ and P-DED. Polyplexes formed with P-DED generally showed higher zeta potentials as compared to all other polymers due to the polymer's high buffering capacity above pH 7.4, which results in

a higher number of protonated amines at pH 7.4 that are available for pDNA complexation (Fig. 3). The zeta potential of all polyplexes formed by the synthesized polymers increased as the weight ratio of polymer to pDNA increased, which corresponds with the increased N:P ratios within the polyplexes.

**Band Retardation with Gel Electrophoresis**—The electrophoretic patterns of the polymer/pDNA polyplexes were obtained by gel electrophoresis (Fig. 7). Lane 8 in all images represents uncomplexed negatively charged pDNA (naked pDNA), which migrated to the positive end of the gels. P-AEPZ and P-DED were able to retard the migration of pDNA at polymer/pDNA weight ratios of 10:1 or higher. P-AEPZ and P-DED neutralized the charges of pDNA at a ratio of 10:1, which is in accordance with the results for the zeta potential measurements (Fig. 6). Polyplexes with P-AEPZ/Hyd and P-API/Hyd, which exhibit lower N:P ratios at a given polymer/pDNA weight ratio, were able to retard the migration of the pDNA at weight ratios of 30:1 or higher and 20:1 or higher, respectively. This is also consistent with the zeta potential data (Fig. 6). Polymers with a higher amount of protonated amine at pH 7.4 (i.e., P-AEPZ and P-DED) were able to retard the migration of pDNA at a lower polymer/pDNA weight ratio.

### Hydrodynamic Size with Dynamic Light Scattering (DLS)

The hydrodynamic size (diameter) of the polyplexes formed at different polymer/pDNA ratios were obtained by DLS (Fig. 8). Naked pDNA had a diameter of  $751.6 \pm 111.8$  nm (data not shown). Upon complexation, the polymer and pDNA yielded condensed particles with a diameter as small as  $111.1 \pm 19.9$  nm (P-DED, polymer/pDNA weight ratio of 500:1). At low polymer/pDNA weight ratios (10:1, 50:1 and 100:1), aggregation of the polyplexes may have occurred as indicated by the large particle diameters ranging from  $832.0 \pm 85.4$  nm to  $1910.5 \pm 17.2$  nm. At low weight ratios, neutrality of the polyplexes may cause particle aggregation as electrostatic repulsion is minimal. The zeta potentials increased as the polymer/pDNA ratios were increased (Fig. 6) and individual polyplexes were electrostatically stabilized<sup>40</sup>. The large particle diameters observed for polyplexes formed with a low polymer/pDNA weight ratio could also have resulted from the inability of the polymers to condense pDNA at low polymer/pDNA weight ratios. Polyplexes formed at a polymer/pDNA weight ratio of 300:1 or higher were significantly smaller in size compared to those formed at a polymer/pDNA weight ratio of 100:1 or lower. Compared to the other polymers, P-DED formed individual particles with small particle diameters even at the lowest polymer/pDNA ratio tested (10:1). Due to the polymer's high buffering capacity above pH 7.4, the formed polyplexes were positively charged even at low weight ratios and were able to repulse each other and avoid aggregation. All synthesized polymers were able to form complexes with and condense pDNA at appropriate N:P ratios, which is beneficial for DNA stabilization and transfection<sup>41</sup>. The polyplexes formed by the synthesized polymers may not be as small as those formed by branched PEI (25 kDa), however, they are still promising for gene delivery. Larger sized particles have been shown to sediment onto cells, which enhances particle uptake by increasing the interaction with the cells in 2D cultures<sup>42,43</sup>. Although P-AEPZ/Hyd and P-API/Hyd form complexes with lower zeta potential compared to P-AEPZ and P-DED (Fig. 6), P-AEPZ/Hyd and P-API/Hyd were able to condense pDNA to low hydrodynamic sizes at high polymer/pDNA weight ratios. There was no increase in surface charge of the polyplexes formed after a certain weight ratio as also observed by other groups in the literature<sup>18</sup>. However, improvement in the condensation of the pDNA was still observed. This suggests that above a certain polymer/pDNA weight ratio, additional polymer may not increase the surface charge of the polyplexes, however, it may still improve pDNA condensation.

**Transfection Efficiency with Enhanced Green Fluorescent Protein Reporter Gene**—The transfection efficiencies of the polyplexes formed by the synthesized polymers

were evaluated using rat fibroblasts as a model cell line and the results are summarized in Figure 9. At low polymer/pDNA weight ratios (10:1, 50:1 and 100:1), the polyplexes formed by the different polymers did not result in significantly higher numbers of transfected cells as compared to naked pDNA. We hypothesized that this resulted from the significantly larger hydrodynamic size of polyplexes formed at the lower polymer/pDNA weight ratios compared to at the higher weight ratios (300:1 and 500:1). The insufficient condensation and stabilization of the pDNA may have led to the lower transfection efficiencies observed<sup>41</sup>. At a polymer/pDNA weight ratio of 300:1, polyplexes formed with P-AEPZ, P-DED and P-AEPZ/Hyd resulted in significantly higher transfection efficiencies ( $11.8 \pm 2.6\%$ ,  $30.6 \pm 6.6\%$  and  $5.3 \pm 1.0\%$ , respectively) than naked pDNA ( $0.8 \pm 0.4\%$ ). At this weight ratio (300:1), polyplexes formed with P-DED, which has the highest number of dissociated amines available for pDNA complexation (Fig. 3), even resulted in a significantly higher transfection efficiency ( $30.6 \pm 6.6\%$ ) than observed for pDNA polyplexes with PEI (weight ratio of 2:1,  $25.5 \pm 2.7\%$ ). Compared to all other synthesized polymers, P-DED had the highest amount of amines that dissociate above pH 7.4 which are available for pDNA complexation. P-DED showed more efficient pDNA complexation and condensation and formed polyplexes with higher zeta potential (Fig. 6). This is especially beneficial for effective interaction with negatively charged cell membranes and cellular uptake. The high transfection efficiencies observed are a good indication that the polyplexes were successfully internalized by the cells and led to expression of GFP. As compared to PEI, a much larger excess of P-DED was required for effective pDNA complexation and cellular transfection, which is explained by the comparatively low molecular weight and low charge density of P-DED<sup>38,44</sup>. Due to the excellent cytocompatibility of P-DED (Fig. 5), such high polymer to pDNA ratios are not a concern.

Fluorescence images were taken to confirm the transfection results obtained by flow cytometry. A set of confocal images of cells treated with plain media was taken as a negative control (Fig. 10A). There was no transfection observed for cells exposed to media containing naked pDNA (Fig. 10B). Cells exposed to polyplexes formed with P-DED at a weight ratio of 300:1 had intense expression of GFP as seen by the bright green fluorescence in Figure 10C. Cells that were transfected with polyplexes formed with PEI (at a weight ratio of 2:1) also showed significant expression of GFP (Fig. 10D), however the fluorescence were not as bright and consistent as observed for transfection with P-DED (Fig. 10C).

Quantitative cytotoxicity evaluation was performed with an MTT assay 2 and 24 h after incubating the cells with the polymers at different concentrations. Although quantitative cytotoxicity evaluation was not performed beyond 24 h after cell treatment with the polymer/pDNA polyplexes, qualitative cytotoxicity evaluation was performed with light microscopy at the end of the transfection experiment. In general, wells treated with polyplexes formed by the synthesized polymers, even at the highest polymer/pDNA weight ratio of 300:1, had a high number of live, well spread cells (data not shown). In contrast, a very low number of live cells was observed in wells exposed to polyplexes formed with PEI. The cytotoxicity observed for PEI has been previously reported and likely resulted from the high MW and charge density of the polymer<sup>38</sup>. Transfection was performed in the absence of serum in this study. However, transfection efficiency can be different with the absence or presence of serum. Future transfection studies *in vivo* in an appropriate animal model will yield a more comprehensive analysis of the transfection capabilities of these polymers.

## Conclusions

In this work different polycationic polymers were synthesized from the triacrylate monomer TMPTA and different amine monomers by Michael addition polymerization. The hypothesis was confirmed that through variations of the amine monomers used in the reaction, the amine group density within the polymers and the basicity and buffering capacity of the polymers can

be controlled. By these properties, parameters that are important in the gene delivery process were significantly influenced. It was found that amines that dissociate above pH 7.4 and are available for pDNA complexation, are a key parameter for effective pDNA condensation and transfection. P-DED, the polymer with the most amines dissociating above physiological pH, formed dense polyplexes of high zeta potential which transfected cells more efficiently than branched PEI under the conditions tested. The evaluation of the different polycationic polymers further showed that the availability of unprotonated amines that can autocatalyze degradation does not exclusively predetermine the polymer degradation rate. All synthesized polymers had low cytotoxicity, which allows their use at high N:P ratios as necessary for the fabrication of polyplexes with effective pDNA complexation and cellular transfection. It is concluded that when designing non-viral vectors, it is important to investigate the amount of amines that dissociate in specific pH ranges relevant for autocatalytic degradation, pDNA complexation and endosomal escape instead of only examining the total amount of amines in the polymer.

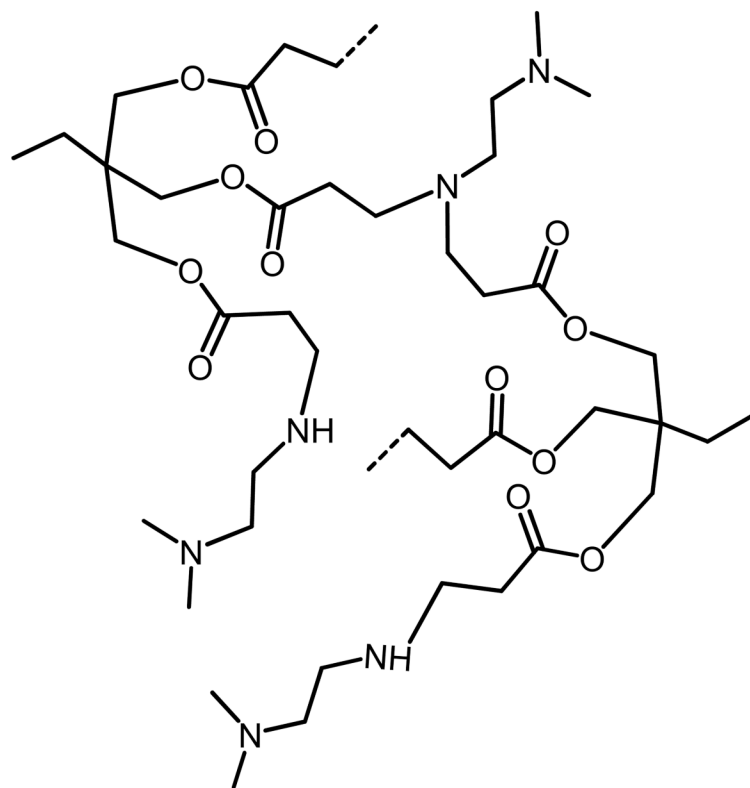
## Acknowledgments

We acknowledge support by a grant from the National Institutes of Health (R21 AR56076). We thank Dr. Joel Moake for the use of the flow cytometer and Dr. Rebecca Richards-Kortum for the use of the DLS instrument. We also thank Dr. Michael R. Diehl, Dr. Ka-Yiu San and Dr. Junghae Suh for the use of their facilities for plasmid DNA amplification.

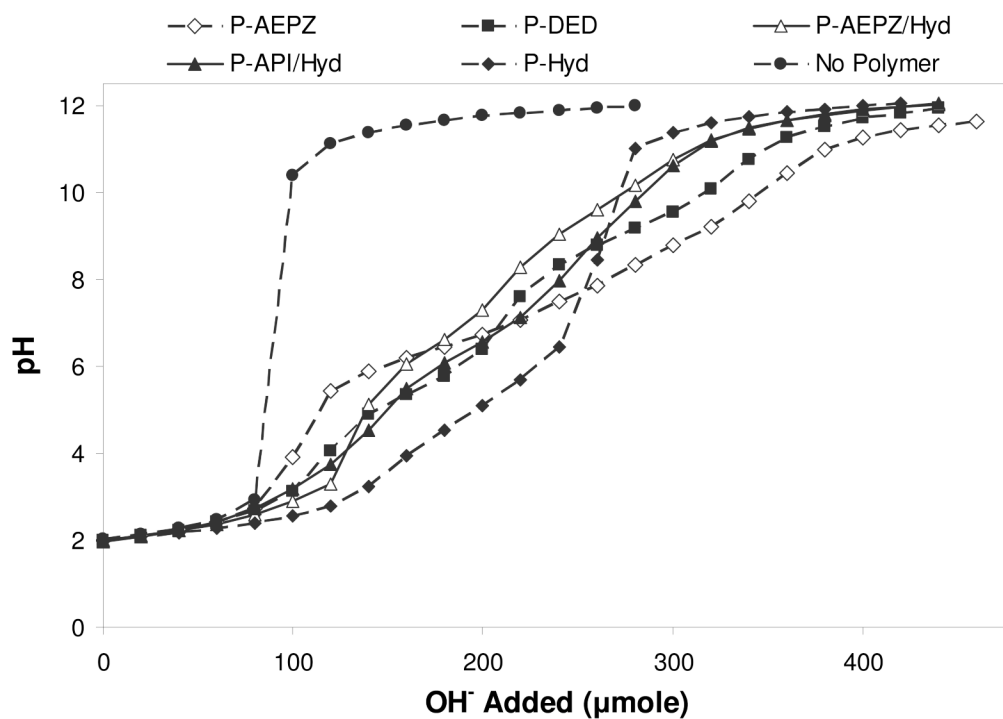
## References

1. Peel AL, Zolotukhin S, Schrimsher GW, Muzyczka N, Reier PJ. *Gene Ther* 1997;4:16–24. [PubMed: 9068791]
2. Reschel T, Konak C, Oupicky D, Seymour LW, Ulbrich K. *J Controlled Release* 2002;81:201–217.
3. Azzam T, Domb AJ. *Curr Drug Delivery* 2004;1:165–193.
4. Putnam D, Gentry CA, Pack DW, Langer R. *Proc Natl Acad Sci USA* 2001;98:1200–1205. [PubMed: 11158617]
5. Brox R, Garipey J. *Methods Mol Med* 2004;90:139–160. [PubMed: 14657563]
6. Tanahashi K, Mikos AG. *J Biomed Mater Res, Part A* 2003;67:1148–1154.
7. Luten J, van Nostrum CF, De Smedt SC, Hennink WE. *J Controlled Release* 2008;126:97–110.
8. Eldred SE, Pancost MR, Otte KM, Rozema D, Stahl SS, Gellman SH. *Bioconjug Chem* 2005;16:694–699. [PubMed: 15898739]
9. Choksakulnimitr S, Masuda S, Tokuda H, Takakura Y, Hashida M. *J Controlled Release* 1995;34:233–241.
10. Breunig M, Lungwitz U, Liebl R, Goepferich A. *Proc Natl Acad Sci USA* 2007;104:14454–14459. [PubMed: 17726101]
11. Zhong Z, Song Y, Engbersen JF, Lok MC, Hennink WE, Feijen J. *J Controlled Release* 2005;109:317–329.
12. Wu DC, Liu Y, Chen L, He CB, Chung TS, Goh SH. *Macromolecules* 2005;38:5519–5525.
13. Wu DC, Liu Y, He CB, Chung TS, Goh ST. *Macromolecules* 2004;37:6763–6770.
14. Lynn DM, Anderson DG, Putnam D, Langer R. *J Am Chem Soc* 2001;123:8155–8156. [PubMed: 11506588]
15. Lynn DM, Langer R. *J Am Chem Soc* 2000;122:10761–10768.
16. Kim TI, Seo HJ, Choi JS, Yoon JK, Baek JU, Kim K, Park JS. *Bioconjug Chem* 2005;16:1140–1148. [PubMed: 16173791]
17. Kim T, Seo HJ, Baek J, Park JH, Park JS. *Bull Korean Chem Soc* 2005;26:175–177.
18. Wu D, Liu Y, Jiang X, Chen L, He C, Goh SH, Leong KW. *Biomacromolecules* 2005;6:3166–3173. [PubMed: 16283742]
19. Chew SA, Hacker MC, Saraf A, Raphael RM, Kasper FK, Mikos AG. *Biomacromolecules* 2009;10:2436–2445. [PubMed: 19678696]
20. You YZ, Manickam DS, Zhou QH, Oupicky D. *J Controlled Release* 2007;122:217–225.
21. Tao L, Liu J, Tan BH, Davis TP. *Macromolecules* 2009;42:4960–4962.

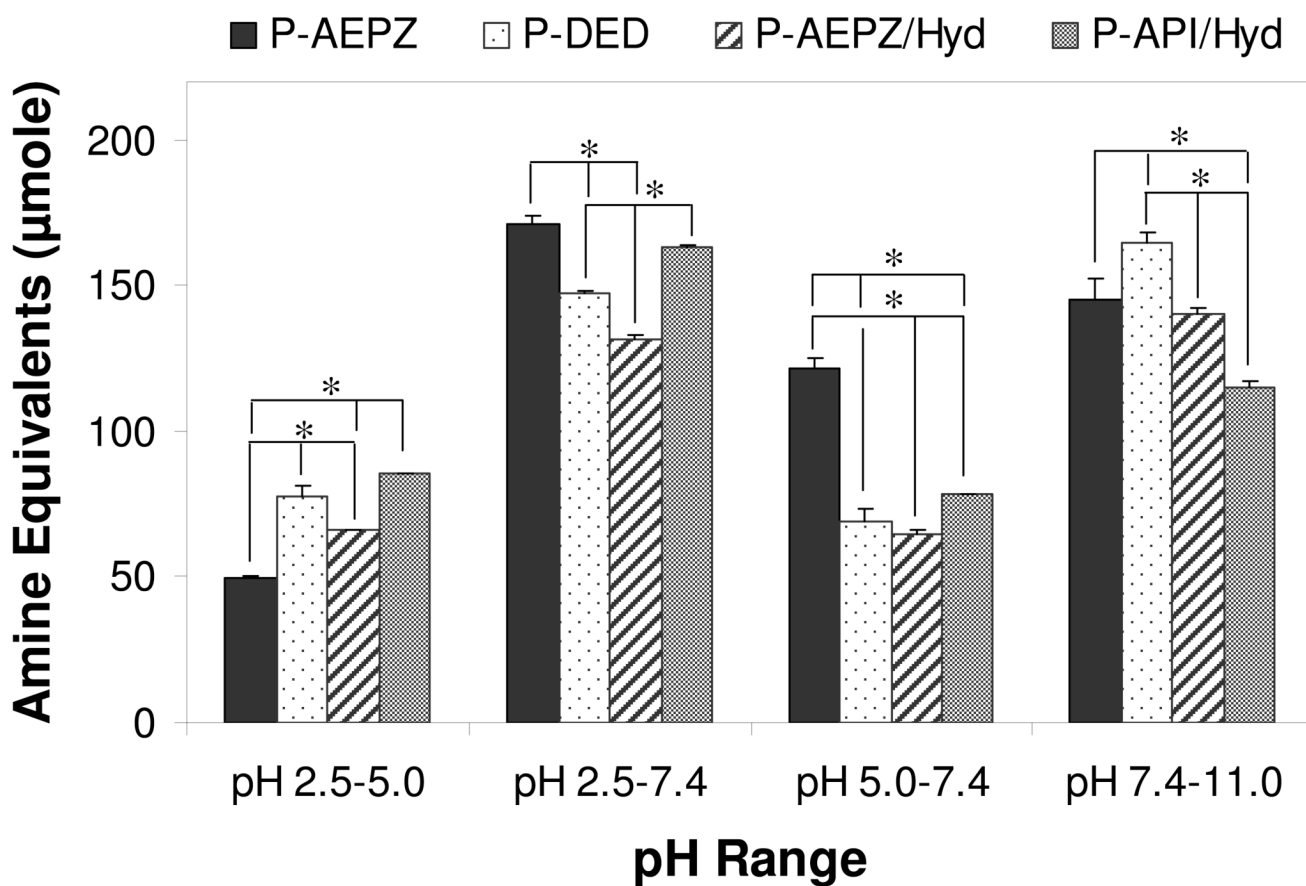
22. Tseng WC, Fang TY, Su LY, Tang CH. *Mol Pharm* 2005;2:224–232. [PubMed: 15934783]
23. Forrest ML, Koerber JT, Pack DW. *Bioconjug Chem* 2003;14:934–940. [PubMed: 13129396]
24. Liu Y, Wu D, Ma Y, Tang G, Wang S, He C, Chung T, Goh S. *Chem Commun* 2003:2630–2631.
25. Lu L, Stamatas GN, Mikos AG. *J Biomed Mater Res* 2000;50:440–451. [PubMed: 10737887]
26. Timmer MD, Shin H, Horch RA, Ambrose CG, Mikos AG. *Biomacromolecules* 2003;4:1026–1033. [PubMed: 12857088]
27. Saraf A, Hacker MC, Sitharaman B, Grande-Allen KJ, Barry MA, Mikos AG. *Biomacromolecules* 2008;9:818–827. [PubMed: 18247565]
28. Hosseinkhani H, Aoyama T, Yamamoto S, Ogawa O, Tabata Y. *Pharm Res* 2002;19:1471–1479. [PubMed: 12425464]
29. Yoshii E. *J Biomed Mater Res* 1997;37:517–524. [PubMed: 9407300]
30. Fischer D, Bieber T, Li Y, Elsasser HP, Kissel T. *Pharm Res* 1999;16:1273–1279. [PubMed: 10468031]
31. Chen QR, Zhang L, Luther PW, Mixson AJ. *Nucleic Acids Res* 2002;30:1338–1345. [PubMed: 11884631]
32. Midoux P, Monsigny M. *Bioconjug Chem* 1999;10:406–411. [PubMed: 10346871]
33. Pack DW, Putnam D, Langer R. *Biotechnol Bioeng* 2000;67:217–223. [PubMed: 10592519]
34. Kanayama N, Fukushima S, Nishiyama N, Itaka K, Jang WD, Miyata K, Yamasaki Y, Chung UI, Kataoka K. *ChemMedChem* 2006;1:439–444. [PubMed: 16892379]
35. Xiong MP, Bae Y, Fukushima S, Forrest ML, Nishiyama N, Kataoka K, Kwon GS. *ChemMedChem* 2007;2:1321–1327. [PubMed: 17579918]
36. Ahlstrom B, Edebo L. *Microbiology* 1998;144(Pt 9):2497–2504. [PubMed: 9782497]
37. Kloeckner J, Bruzzano S, Ogris M, Wagner E. *Bioconjug Chem* 2006;17:1339–1345. [PubMed: 16984145]
38. Breunig M, Lungwitz U, Liebl R, Fontanari C, Klar J, Kurtz A, Blunk T, Goepferich A. *J Gene Med* 2005;7:1287–1298. [PubMed: 15906395]
39. Tanahashi K, Jo S, Mikos AG. *Biomacromolecules* 2002;3:1030–1037. [PubMed: 12217050]
40. Anwer K, Rhee BG, Mendiratta SK. *Crit Rev Ther Drug Carrier Syst* 2003;20:249–293. [PubMed: 14635981]
41. Holtorf, HL.; Mikos, AG. *Pharmaceutical Perspectives of Nucleic Acid-Based Therapeutics*. K, SW., editor. Taylor & Francis; New York: 2002. p. 367-387.
42. Boussif O, Zanta MA, Behr JP. *Gene Ther* 1996;3:1074–1080. [PubMed: 8986433]
43. Ogris M, Steinlein P, Kursa M, Mechtler K, Kircheis R, Wagner E. *Gene Ther* 1998;5:1425–1433. [PubMed: 9930349]
44. Godbey WT, Wu KK, Mikos AG. *J Biomed Mater Res* 1999;45:268–275. [PubMed: 10397985]



**Figure 1.** General structure of a branched polymer obtained by Michael addition reaction of TMPTA with an amine monomer (shown here: DED).



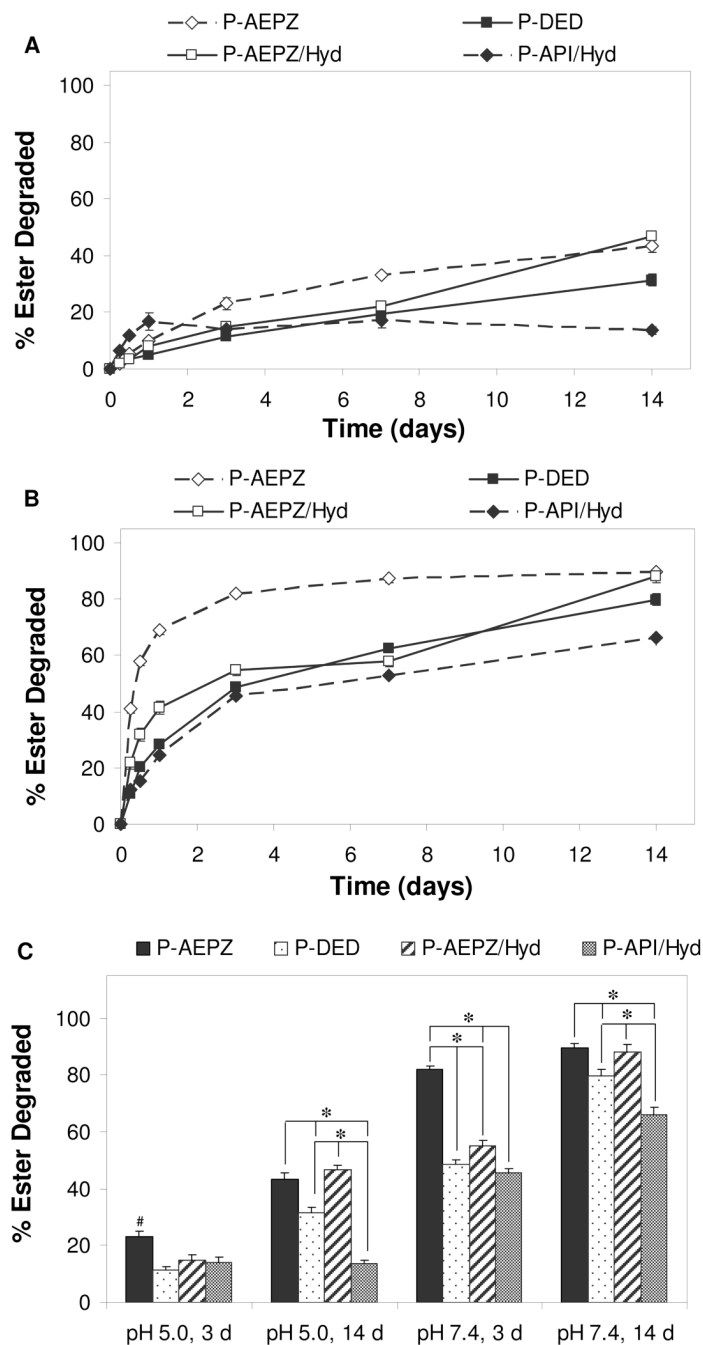
**Figure 2.** Titration curves (0.1 N NaOH) of the different polymers. Values for P-AEPZ are adopted from a previous study<sup>19</sup>. The results are expressed as means  $\pm$  standard deviations for  $n=3$ .



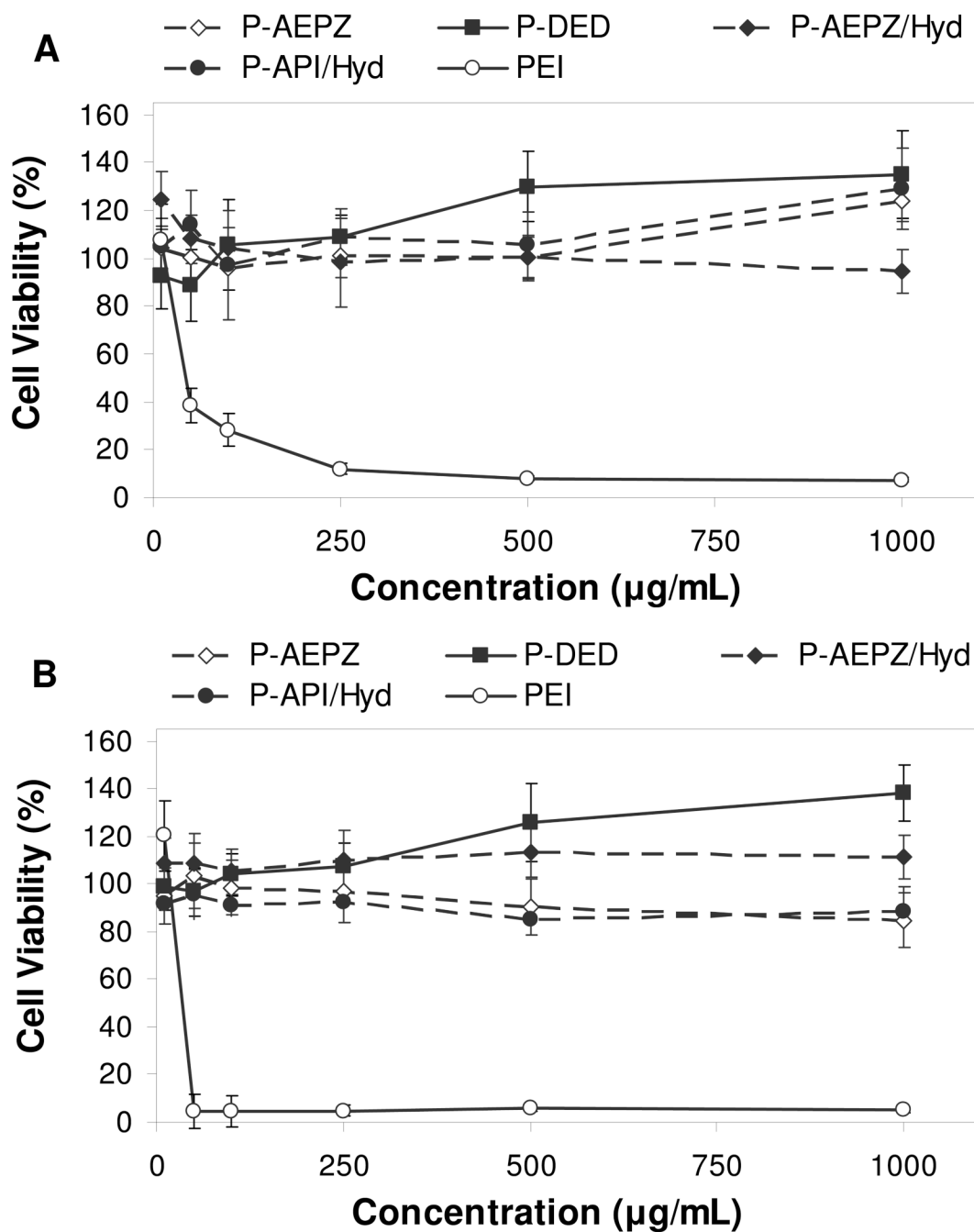
**Figure 3.**

Amine equivalents that dissociate within different pH ranges. The results represent means  $\pm$  standard deviations for  $n=3$ . # indicates a statistically significant difference between one polymer and all other polymers within the same pH interval ( $p<0.05$ ). Values for P-AEPZ are adopted from a previous study<sup>19</sup>. \* represents a statistically significant difference between two polymers within the same pH interval ( $p<0.05$ ).

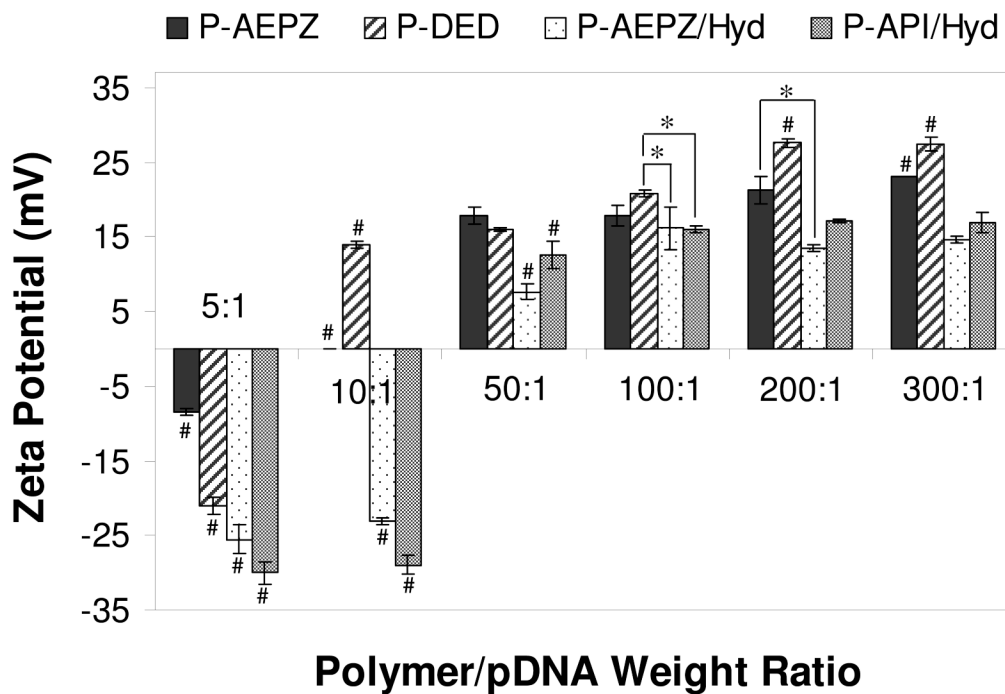




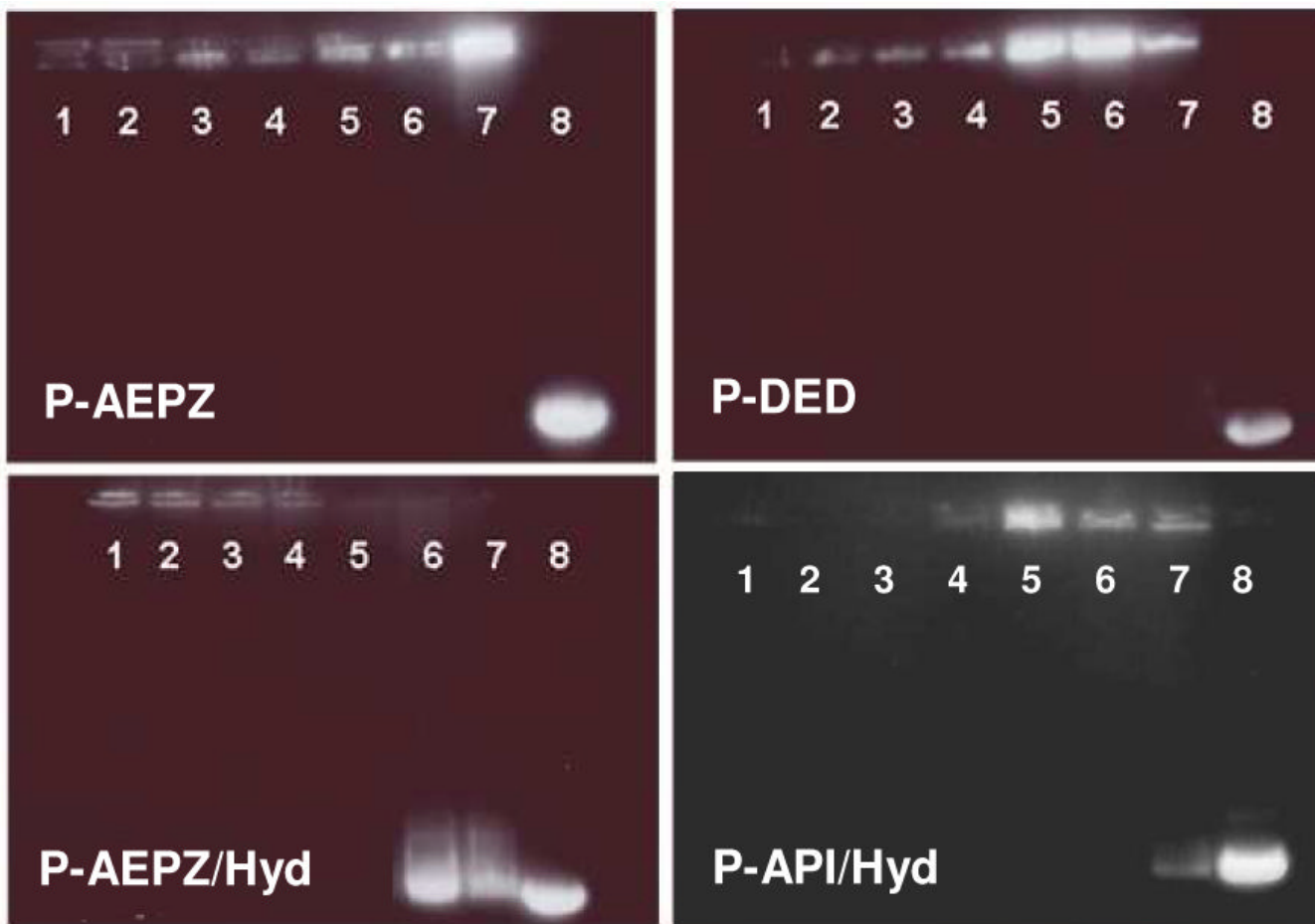
**Figure 4.** Ester degradation profiles of the different polymers at 37°C and (A) pH 5.0 simulating lysosomal pH and (B) pH 7.4 simulating cytoplasmic pH and (C) degree of degradation after 3 and 14 days at pH 5.0 and 7.4 at 37°C as observed by  $^1\text{H-NMR}$ . The extent of degradation is expressed as means  $\pm$  standard deviation for  $n=3$ . # indicates a statistically significant difference between one polymer and all other polymers degraded under the same conditions ( $p<0.05$ ). Values for P-AEPZ are adopted from a previous study<sup>19</sup>. \* represents a statistically significant difference between two polymer compositions degraded under the same conditions ( $p<0.05$ ).



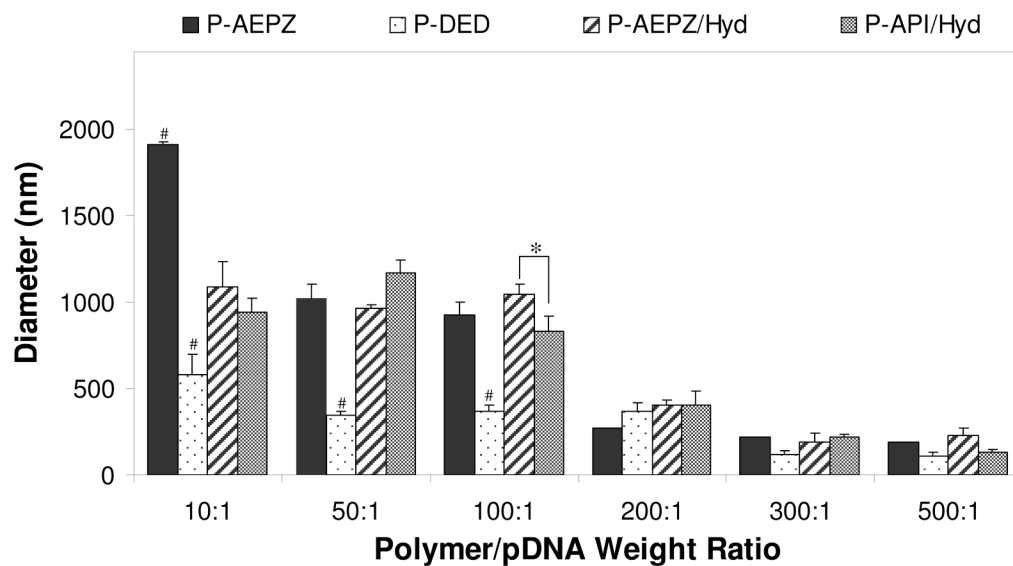
**Figure 5.** Cytotoxicity of the different polymers with polyethylenimine (PEI; 25kDa) as negative control on CRL 1764 rat fibroblasts after (A) 2 h and (B) 24 h as evaluated by a MTT assay. The results are expressed as means  $\pm$  standard deviation for  $n=5$ .



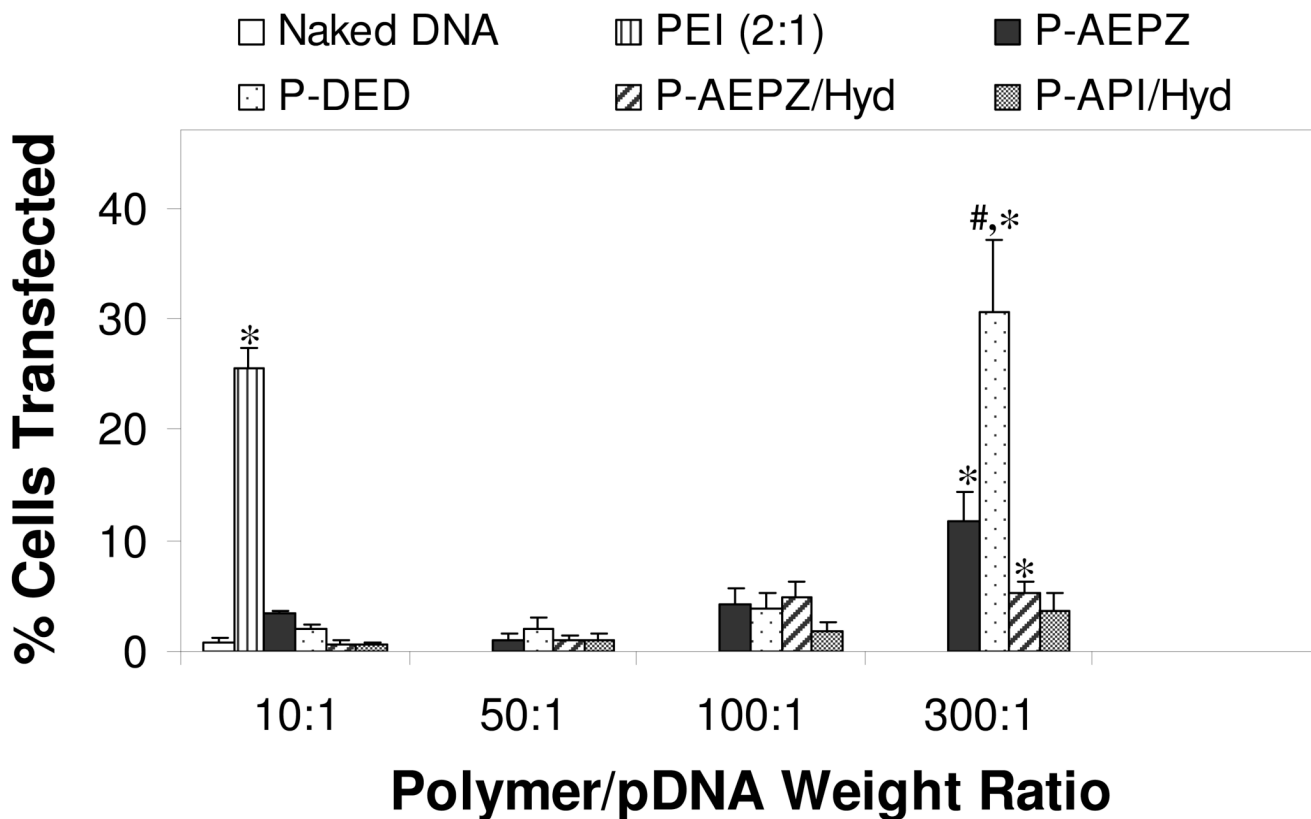
**Figure 6.** Zeta potential of the polyplexes formed with 10  $\mu$ g pCMV-eGFP DNA at different polymer/pDNA weight ratios. The results are expressed as means  $\pm$  standard deviation for  $n = 3$ . # indicates statistically significant difference between a polyplex and all other polyplexes formed at the same weight ratio ( $p < 0.05$ ). Values for P-AEPZ are adopted from a previous study<sup>19</sup>. \* represents a statistically significant difference between two polyplexes formed at the same weight ratio ( $p < 0.05$ ).



**Figure 7.** Gel retardation assay of pDNA/polymer polyplexes at different polymer/pDNA weight ratios: (1) 100:1, (2) 80:1, (3) 60:1, (4) 40:1, (5) 30:1, (6) 20:1, (7) 10:1, and (8) naked pDNA. Results for P-AEPZ are adopted from a previous study<sup>19</sup>.

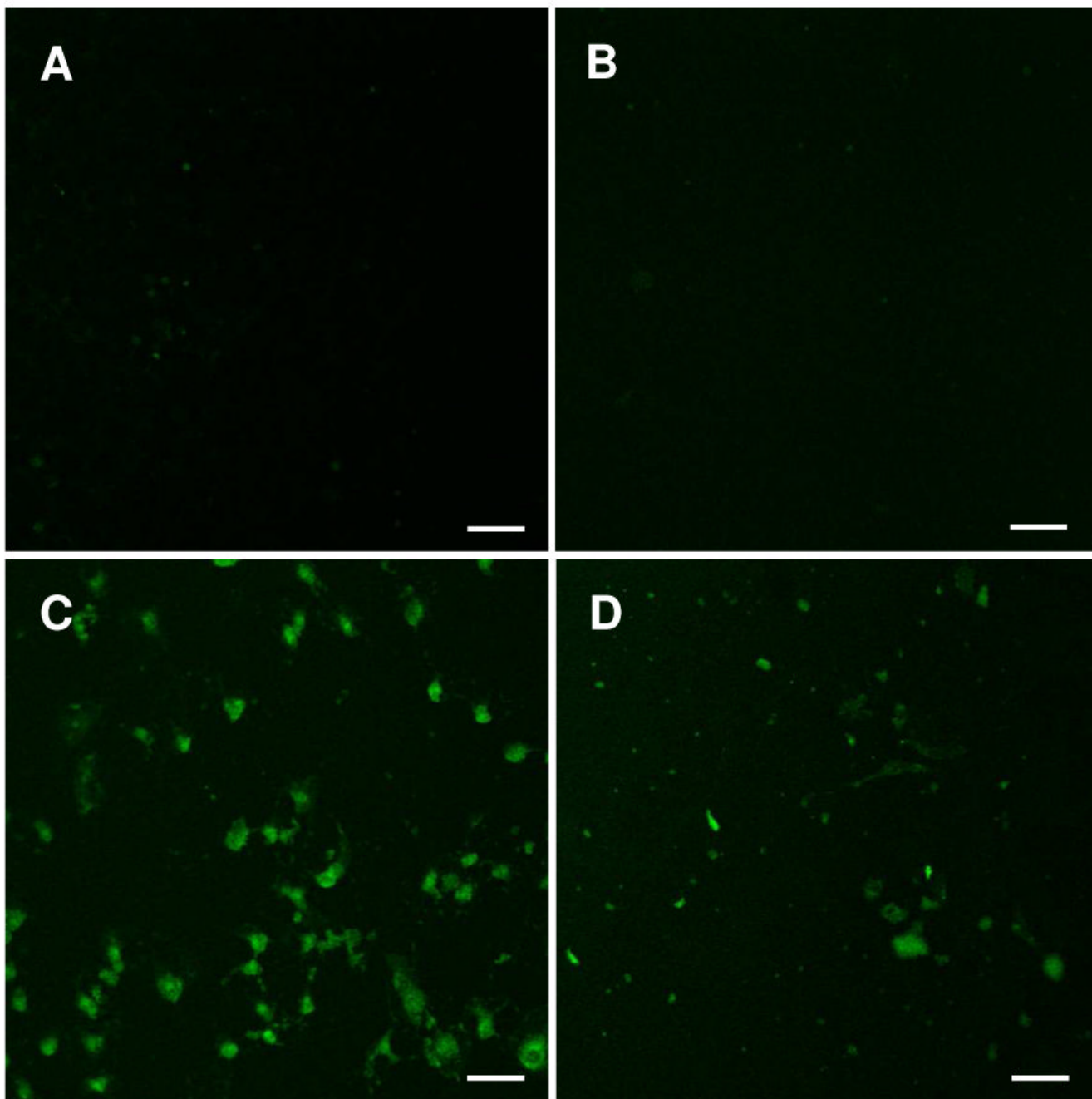


**Figure 8.** Diameter of the polyplexes formed with 10 µg pCMV-eGFP DNA at different polymer/pDNA weight ratios as evaluated by DLS. The results are expressed as means  $\pm$  standard deviation for  $n=3$ . # indicates statistically significant difference between a polyplex formulation and polyplexes formed by all other polymers of the same weight ratio ( $p<0.05$ ). Values for P-AEPZ are adopted from a previous study<sup>19</sup>. \* represents a statistically significant difference between polyplexes of the same weight ratio ( $p<0.05$ ).



**Figure 9.**

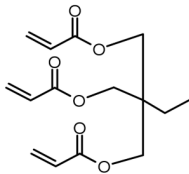
Efficiency of CRL 1764 cell transfection with polyplexes formed from 5 µg pCMV-eGFP DNA at different polymer/pDNA weight ratios. Naked pDNA and polyplexes formed by PEI at a polymer/pDNA weight ratio of 2:1 served as controls. The results are expressed as means  $\pm$  standard deviation for  $n = 4-6$ . \* indicates a statistically significant difference between a polyplex and naked pDNA ( $p < 0.05$ ). # indicates a statistically significant increased transfection efficacy as compared to the transfection efficacy of PEI/pDNA polyplexes ( $p < 0.05$ ).



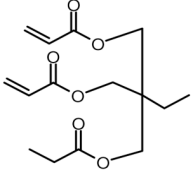
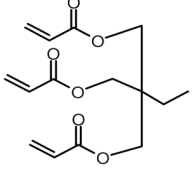
**Figure 10.** Representative fluorescence images of CRL 1764 cells after exposure to the following media: (A) plain medium, (B) naked pDNA (CMV-eGFP), (C) P-DED/pDNA (300:1), and (D) PEI/pDNA (2:1). In groups B-D, 5  $\mu$ g pCMV-eGFP DNA were used. Green fluorescence in cells represents expression of GFP.

**Table 1**

Polymer composition and structures of the triacrylate and amine monomer building blocks. P-AEPZ, P-DED, P-AEPZ/Hyd and P-API/Hyd vary in types of amines they consist of.

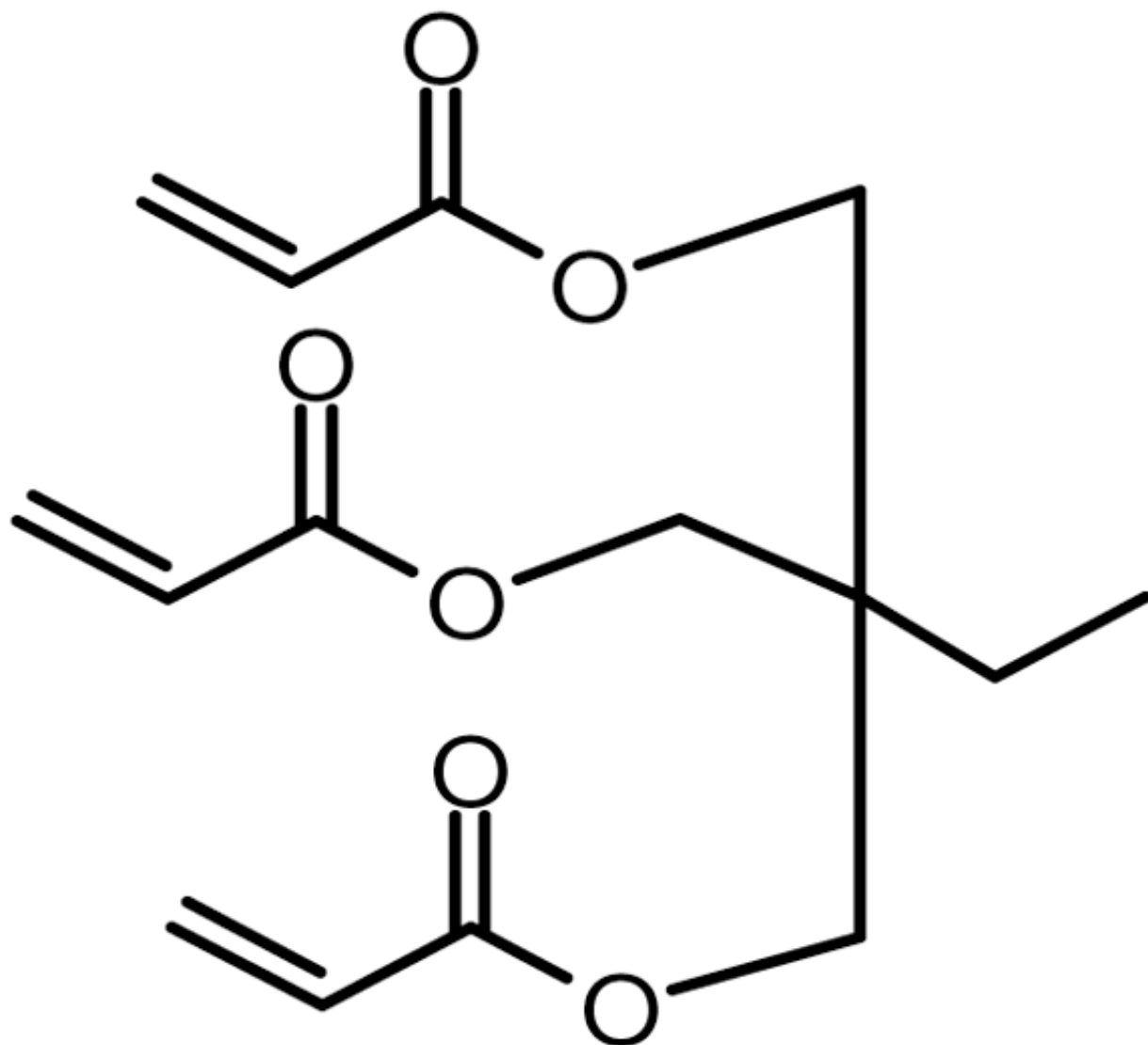
| Group  | Triacrylate Monomer   |
|--------|---|
| P-AEPZ |  <p data-bbox="943 1136 1032 1161">TMPTA</p> |



| Group | Triacrylate Monomer   |
|-------|---|
| P-API |  <p data-bbox="943 600 1037 638">TMPTA</p>    |
| P-DED |  <p data-bbox="943 1083 1037 1121">TMPTA</p> |

Group

Triacrylate Monomer

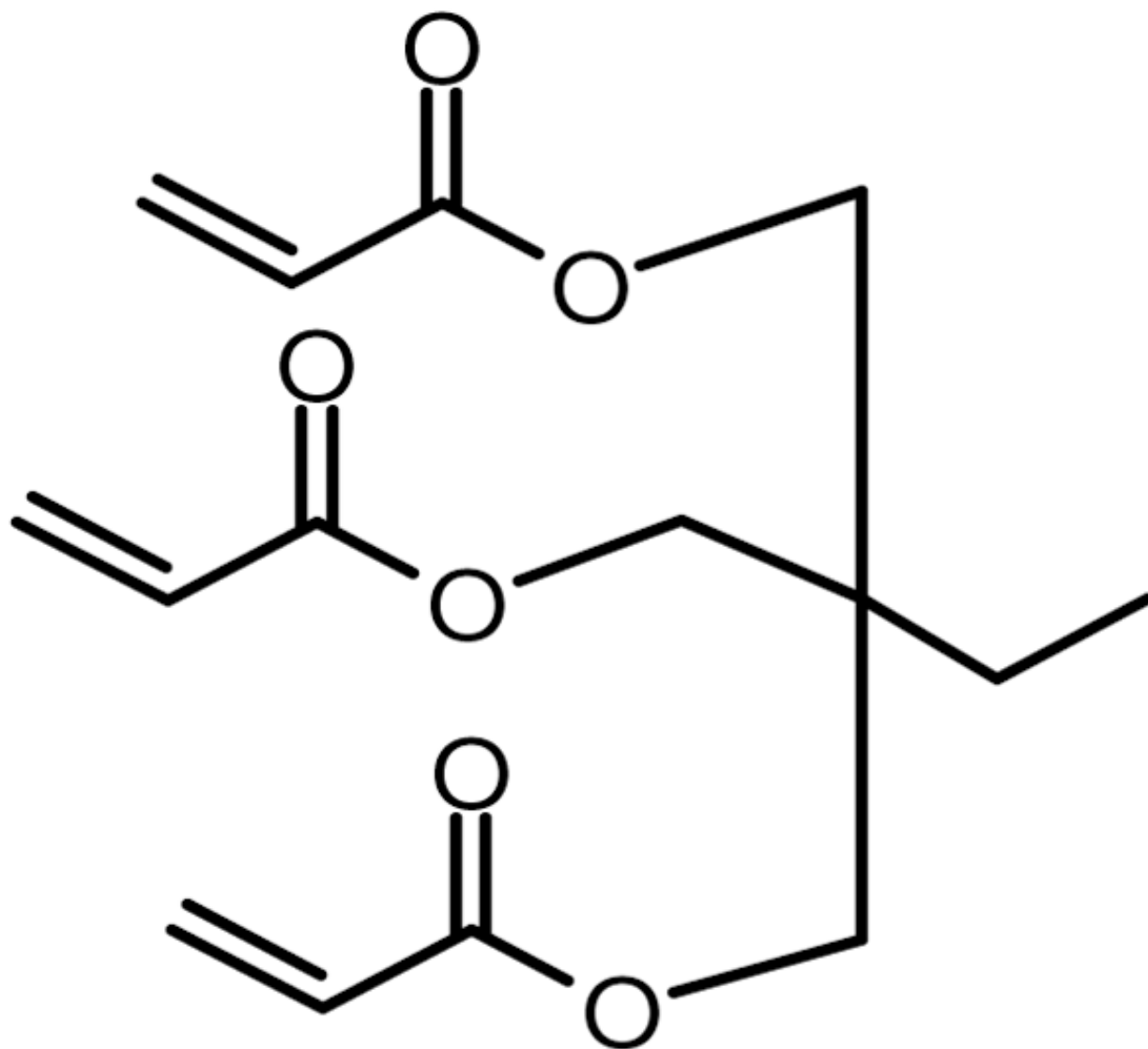


P-Hyd

**TMPTA**

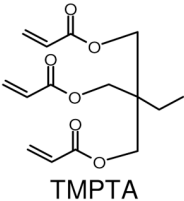
Group

Triacrylate Monomer



P-AEPZ/Hyd

**TMPTA**

| Group     | Triacrylate Monomer   |
|-----------|---|
| P-API/Hyd |  <p>TMPTA</p> |

**Table 2**

Number average molecular weight, weight average molecular weight, polydispersity index (PDI), estimated average number of triacrylate and amine monomers per polymer molecule and pKa values of the different polymers examine in this study. Values for P-AEPZ are adopted from a previous study<sup>19</sup>.

| Polymer    | Mn (Da)* | Mw (Da)* | PDI* | Number of Triacrylate Monomers <sup>†</sup> | Number of Amine Monomers <sup>†</sup> | pKa <sub>1</sub> <sup>#</sup> | pKa <sub>2</sub> <sup>#</sup> | pKa <sub>3</sub> <sup>#</sup> |
|------------|----------|----------|------|---|---------------------------------------|-------------------------------|-------------------------------|-------------------------------|
| P-AEPZ     | 2700     | 6671     | 2.47 | 4 (10)                                      | 8 (20)                                | 7.85                          | -                             | -                             |
| P-DED      | 838      | 946      | 1.13 | 2 (2)                                       | 4 (4)                                 | 5.56                          | 9.56                          | -                             |
| P-Hyd      | -        | -        | -    | -   | -                                     | 4.24                          | -                             | -                             |
| P-AEPZ/Hyd | 812      | 888      | 1.09 | 2 (2)                                       | 4 (4)                                 | 6.34                          | 9.61                          | -                             |
| P-API/Hyd  | 796      | 840      | 1.06 | 2 (2)                                       | 4 (4)                                 | 4.14                          | 6.32                          | 8.96                          |

\* Measured by size exclusion chromatography

<sup>†</sup> Estimated from number average molecular weight; numbers in parentheses estimated from weight average molecular weight

<sup>#</sup> Determined from titration curve